

Technical paper to be presented at the ASHRAE 1990 Winter Meeting, February 11-14, Atlanta Georgia. To be published in 1990 ASHRAE Transactions.

THEORETICAL AND COMPUTATIONAL INVESTIGATION OF SIMULTANEOUS HEAT AND MOISTURE TRANSFER IN BUILDINGS: "EFFECTIVE PENETRATION DEPTH" THEORY

Alp Kerestecioglu (Member)
Muthusamy Swami
Adel Kamel (Student Member)

ABSTRACT

Several approaches can be taken in studying the combined heat and moisture transport characteristics of building materials. The "effective moisture penetration depth" (EMPD) approach described in this paper is a simplified method of analyzing moisture transport in buildings, and is easy to incorporate into existing building energy analysis computer codes. First, the paper introduces the building domains and explains the lumped heat and moisture balance equations for the room air. The components of the moisture balance equation involving moisture adsorption and desorption are described in detail where the concept of EMPD is discussed. The assumptions, parameters required and limitations of the model are also discussed. Results of simulation using the model and comparison with measured data are given. Data of isotherms compiled from the literature of some commonly used building materials are also given.

While results show that the EMPD model is a viable approach to building energy analysis, the model must be used with caution and good judgement. Experimental data and/or distributed analysis using the detailed moisture transport equations to determine the limits of its applicability in terms of operating conditions and material types, are needed.

A. Kerestecioglu is a Research Associate; M. Swami, Research Engineer; A. Kamel, Graduate Research Assistant, Research and Development Division of the Florida Solar Energy Center, 300 State Road 401, Cape Canaveral, FL 32920.

INTRODUCTION

In humid climates, one of the major loads in air-conditioned buildings is due to moisture. If alternative energy solutions are to be sought for cooling and dehumidification, it is imperative to understand and model moisture transport correctly. Moisture has little effect on heating system performance but a profound effect on the performance of air-conditioning systems. If it is assumed that all moisture is contained in the room air, one is ignoring the fact that the materials which bound the room (e.g. wall surfaces, furnishings, and linens) have the capability to store and release moisture. This assumption is false and can lead to significant error in the prediction of room moisture conditions and cooling loads. In addition, the study of innovative cooling and dehumidification systems requires that analytical assessments of proposed concepts be performed if research is to be cost effective. Without an accurate tool, such studies simply cannot be performed.

In building simulations, predicting the indoor conditions and the associated loads are the central issues. To do this, the transport equations must be solved for each building component. In general a transport equation can be written in either lumped or distributed form. If some building components can be defined by lumped equations and others by distributed equations, the problem is not continuous, and separate domains must be considered.

For mathematical convenience the building is divided into three domains and three boundaries which separate these domains as shown in Figure 1. The building domains and their characteristics are given in Table 1. If the whole building is represented with distributed equations, the problem can be solved as a continuum, and only one domain is needed. However, in this case, the fluid flow equations must be solved in detail for the air domain. Currently, this is not

a practical approach; therefore, most of the simulations in the buildings area use lumped equations for the air domain. The solid domains can be solved either by the lumped or distributed approaches. Mathematically, this choice depends on the Biot number (ratio of solid side resistance to fluid side resistance). If this number is low (less than 0.1), lumped equations may be used. If the heat and mass Biot numbers, [$Bi_T = h_T L / k$ and $Bi_M = h_M L / (\rho_a D_v)$], are calculated based on the full thickness of the material, lumped equations may not be used. However, this study considers a thin layer (1 to 5 mm) adjacent to the surface, and assumes all moisture interactions take place in this layer. Consequently, the characteristic length, L , to be used in calculation of Biot numbers is very small. If the inner regions of the material is participating in mass exchange (long time storage in the order of days) this concept may fail.

Substantial work in lumped analysis has been performed by Cunningham (1983.a; 1983.b; 1984; 1988). Cunningham developed a model using adjusted convective mass transfer coefficients, that would calculate the moisture concentration of a building cavity containing hygroscopic material. Similar models with similar assumptions were also used by Cleary and Sonderegger (1984), Burch (1985), Cleary (1985), and Cleary and Sherman (1985) for predicting performance of attics. However, their studies used actual convective mass transfer coefficients and full material thicknesses. Kusuda (1983) and Kusuda and Miki (1985) again used a similar model for estimating the indoor humidity levels. In their study of a Japanese test house, they determined the existence of a boundary layer approximately 4 mm thick in solid surface that was affected by the diurnal changes in room air conditions.

In lumped moisture models, a number of parameters can be effectively "adjusted" by the analyst. Many analysts choose to determine an "effective" convective mass

transfer coefficient from experimental results and use actual thicknesses, surface areas, and moisture isotherms in the solution schemes. This study uses "actual" convective mass transfer coefficients that are determined via existing heat and mass transfer relationships (e.g. the Lewis relation). Preferring to use actual surface areas and moisture sorption isotherms, the study determines an "effective moisture penetration depth" (EMPD) from either experimental or detailed simulation data, and represents the moisture capacity of the problem using a "lump" of this thickness.

MATHEMATICAL FORMULATIONS

In this section the lumped heat and moisture transfer equations for multiple connected air domains are given. The air domain is assumed to be well mixed and the word "zone" is used to indicate the air domain. The governing balance equations in a given "zone," i , may be written as:

Energy Balance:

$$\begin{aligned}
 (\rho_a V C_p)_i \, dTr_i/d\tau = & Q_{\text{equ-}s_i} + Q_{\text{fur-}s_i} + Q_{\text{inf-}s_i} + Q_{\text{lig-}s_i} + Q_{\text{mix-}s_i} + \\
 & Q_{\text{peo-}s_i} + Q_{\text{sin-}s_i} + Q_{\text{sor-}s_i} + Q_{\text{sup-}s_i} + Q_{\text{ven-}s_i} + \\
 & Q_{\text{wal-}s_i} \quad \text{in } \Omega_a
 \end{aligned} \quad (1)$$

Moisture Balance:

$$\begin{aligned}
 (\rho_a V)_i \, dWr_i/d\tau = & Q_{\text{con-}l_i} + Q_{\text{equ-}l_i} + Q_{\text{fur-}l_i} + Q_{\text{inf-}l_i} + Q_{\text{mix-}l_i} + \\
 & Q_{\text{peo-}l_i} + Q_{\text{rev-}l_i} + Q_{\text{sin-}l_i} + Q_{\text{sor-}l_i} + Q_{\text{sup-}l_i} + \\
 & Q_{\text{ven-}l_i} + Q_{\text{wal-}l_i} \quad \text{in } \Omega_a
 \end{aligned} \quad (2)$$

The significance of each term on the right-hand side of Eqs. (1) and (2) are given in Tables 2 and 3, respectively. From the solution of Eqs. (1) and (2), the indoor temperature, Tr , and the indoor humidity ratio, Wr , can be calculated. However, the furniture and wall terms (see Tables 2 and 3) in these equations contain additional unknowns, namely the surface temperatures and "surface-air" humidity ratios, associated with Γ_a and Γ_f . Consequently, more equations are

needed in order to obtain a closure to the system of equations.

"EFFECTIVE PENETRATION DEPTH"

The concept of EMPD and lumped analysis is shown in Figure 2. Figures 2.(a) and 2.(b) depict a hypothetical drying stage of a specimen placed in a dry environment. In the early stages of drying, the moisture content of the inner regions of the specimen remains unaffected by the environmental conditions. However, a thin layer (δ_M) close to the surface behaves dynamically and loses moisture to the environment. If the specimen is left in the same environment for a long time, the inner regions of the specimen are also affected. However, for short periods (in the order of few hours) where the cyclic integral of the total moisture adsorption and desorption is zero, the EMPD concept can be used. In other words, the following constraint must be met:

$$\int_r^{r+\Delta r} dU/dr \approx 0 \quad (3)$$

In Eq. (3), Δr denotes a finite time interval where Eq. (3) holds. As shown in Figure 2.(b), the moisture content of this layer is uniform and is discontinuous between the inner regions and this thin layer. However, the following condition is satisfied at each discrete time interval (within each simulation time step):

$$\int_0^L U(x) dx = U \delta_M \quad \text{for all } r$$

The lumped energy and mass transfer equations for the i -th solid domain are given by:

$$(A\rho_s\delta_T C_p)_i dT_i^*/dr = h_{T,i} A_i (T_r - T_i^*) + \lambda h_{M,i} A_i (W_r - W_i^*) + \sum_{j=1}^{nos} \sigma F_{i-j} A_i (T_j^4 - T_i^{*4}) + q''_T A_i \quad \text{in } \Omega_F \quad (4)$$

$$(A\rho_s\delta_M)_i dU_i/dr = \begin{cases} h_{M,i} A_i (W_\alpha - W_i^*) & \text{in } \Omega_F \text{ and } \Omega_e \text{ towards } \Gamma_e \\ h_{M,i} A_i (W_r - W_i^*) & \text{in } \Omega_F \text{ and } \Omega_e \text{ towards } \Gamma_a \end{cases} \quad (5)$$

where δ_T and δ_M are the empirically determined "effective penetration depths" for the thermal and moisture interactions, respectively. Close examination of Eqs. (4) and (5) reveals that the system of equations does not close. The field variables are the temperature, T^* , the moisture content, U , and the "surface-air" humidity ratio, W^* , [note that the "zone" temperature, T_r , and zone humidity ratio, W_r , are given by Eqs. (1) and (2)]. Consequently, a third relation between W^* and U is necessary.

This third relation must be expressed in terms of the "surface-air" humidity ratio and the moisture content. The sorption isotherm may be used for this purpose by expressing the moisture content in terms of T^* and W^* rather than relative humidity. For most building applications, however, the sorption isotherm of the furnishings is unknown. Conceivably, it could be experimentally determined but that would require an almost infinite number of tests to characterize all potential building furnishings and combinations thereof.

If actual sorption isotherm data are not available, a fictitious sorption isotherm may be used to reasonably relate the "surface-air" humidity ratio to the moisture content. Consequently, an error in the approximation of a sorption isotherm for the furnishings can be compensated by the EMPD term if experimental data are available. For most of the building materials the equilibrium moisture sorption isotherm can be defined with the following equation (Kerestecioglu et al. 1988):

$$U = a \phi^b + c \phi^d \quad (6)$$

where

$$\phi = W^*/W_{sat}^* \quad \text{and} \quad W^* = \phi W_{sat}^* \quad (7)$$

and

$$W_{sat}^* = 1/(R_v \rho_a T^*) \exp[23.7093 - 4111/(T^* - 35.45)] \quad (8)$$

Worldwide sorption isotherm data for various building materials are compiled and reduced to the format given by Eq. (6) in Kerestecioglu et al. (1988).

With a known moisture content, U , Eq. (6) can be solved for the relative humidity, ϕ , (relative humidity in this paper is defined in decimal form). Since the relative humidity cannot be explicitly calculated from Eq. (6), the Newton-Raphson iterative technique is used. The relative humidity can be found iteratively using the following equation:

$$\phi_{n+1} = \phi_n - \frac{a \phi_n^b + c \phi_n^d - U}{a b \phi_n^{b-1} + c d \phi_n^{d-1}}$$

With a known surface temperature, T^* , the humidity ratio at saturation can be calculated from Eq. (8). Finally, with a known "surface-air" relative humidity and humidity ratio at saturation, the "surface-air" humidity ratio can be estimated from Eq. (7). For instance, if in Eq. (6) b is set to zero, the relation between U and W^* can be expressed as:

$$W^* = \frac{1}{R_v \rho_a T^*} \exp\left(23.7093 - \frac{4111}{T^* - 35.45}\right) \left(\frac{U - a}{c}\right)^{1/d} \quad (9)$$

The energy equation for the envelope is the well-known conduction equation and is given by:

$$(\rho_s C_p) \partial T / \partial \tau = \nabla \cdot (k \nabla T) \quad \text{in } \Omega_e \quad (10)$$

with the boundary condition:

$$\begin{aligned} & - q''_T + h_T (T^* - T_\alpha) + \epsilon \sigma (T^{*4} - T_s^4) + \lambda h_M (W^* - W_\alpha) \quad \text{on } \Gamma_e \\ - k \nabla T = & \\ & - q''_T + h_T (T^* - T_r) + \sum_{j=1}^{nCS} \sigma F_{i-j} (T^{*4} - T_j^4) + \lambda h_M (W^* - W_r) \quad \text{on } \Gamma_a \end{aligned} \quad (11)$$

The thermal radiation among internal surfaces is simulated through the script-F, F_{i-j} , concept, which is a function of the surface emissivity and the geometric configuration factor (Kerestecioglu et al. 1988).

NUMERICAL SOLUTIONS

The equations to be solved, the field variables to be calculated and the closure requirement of each equation are shown in Table 4. For a single "zone," Eqs. (1), (2), (4), (5) and (6) can be rearranged as shown in the following equations:

$$dT_r/d\tau + P_1(\tau) T_r = Q_1(\tau) \quad (12)$$

$$dW_r/d\tau + P_2(\tau) W_r = Q_2(\tau) \quad (13)$$

$$dT_{i,i}^*/d\tau + P_{3,i}(\tau) T_{i,i}^* + R_{3,i}(\tau) W_{i,i}^* = Q_{3,i}(\tau) \quad (14)$$

$$dU_{i,i}/d\tau + P_{4,i}(\tau) W_{i,i}^* = Q_{4,i}(\tau) \quad (15)$$

$$U_{i,i} + P_{5,i}(\tau) W_{i,i}^* = Q_{5,i}(\tau) \quad (16)$$

Equation (16) is obtained by substituting Eqs. (7) and (8) into Eq. (6) and, also by substituting 0 and 1 for b and d, respectively. The time dependent parameters used in Eqs. (12) through (16) are defined as shown in the following equations:

$$P_1(\tau) = 1/(\rho_a V C_p) (V EI \rho_a C_p + m \cdot C_p + \epsilon_V V EV \rho_a C_p + \sum_{k=1}^{nof+nos} h_{T,k} A_k)$$

$$Q_1(\tau) = 1/(\rho_a V C_p) (Q_{equ-s} + V II \rho_a C_p T_\alpha + Q_{lig-s} + Q_{peo-s} + Q_{sin-s} + Q_{sor-s} + m \cdot C_p T_s + \epsilon_V V IV \rho_a C_p T_\alpha + \sum_{k=1}^{nof+nos} h_{T,k} A_k T_k^*)$$

$$P_2(\tau) = 1/(\rho_a V) (V EI \rho_a + m \cdot + \epsilon_V V EV \rho_a + \sum_{k=1}^{nof+nos} h_{M,k} A_k)$$

$$Q_2(\tau) = 1/(\rho_a V) (Q_{equ-l} + V II \rho_a W_\alpha + Q_{peo-l} + Q_{rev-l} + Q_{sin-l} + Q_{sor-l} + m \cdot W_s + \epsilon_V V IV \rho_a W_\alpha + \sum_{k=1}^{nof+nos} h_{M,k} A_k W_k^*)$$

$$P_{3,i}(\tau) = 1/(A \rho_s \delta_T C_p)_i (h_{T,i} A_i + \sum_{j=1}^{nos} \sigma F_{i-j} T_i^{*3}) \quad R_{3,i}(\tau) = \lambda h_{M,i} A_i / (A \rho_s \delta_T C_p)_i$$

$$Q_{3,i}(\tau) = 1/(A \rho_s \delta_T C_p)_i (h_{T,i} A_i T_r + \lambda h_{M,i} A_i W_r + \sum_{j=1}^{nos} \sigma F_{i-j} T_j^4 + q''_T)$$

$$P_{4,i}(\tau) = \frac{h_{M,i} A_i}{(A\rho_s\delta_M)_i} \quad Q_{4,i}(\tau) = P_{4,i}(\tau) W_r \quad P_{5,i}(\tau) = -\frac{c_i}{W_{sat}^*} \quad Q_{5,i}(\tau) = a_i$$

For each "zone" there is one energy balance equation [Eq. (12)], one moisture balance equation [Eq. (13)], "nof" energy balance equations for the furniture [Eq. (14)], "nof + nos" moisture balance equations for the furniture and envelope [Eqs. (15) and (16)], and "nos" energy equations for the envelope [Eq. (10)]. The "zone" energy and moisture balance equations can be analytically solved, and the analytical solutions are given by:

$$T_r(\tau) = Q_1(\tau)/P_1(\tau) + [T_{ro} - Q_1(\tau)/P_1(\tau)] \exp[-P_1(\tau)\tau]$$

$$W_r(\tau) = Q_2(\tau)/P_2(\tau) + [W_{ro} - Q_2(\tau)/P_2(\tau)] \exp[-P_2(\tau)\tau]$$

Equations (14), (15) and (16) constitute a set of nonlinear algebraic equations, and there are several ways of solving them. Ortega and Rheinboldt (1980) provide an excellent survey of available procedures. Equation (10) is a partial differential equation and can be solved by finite element or finite difference methods. For linear problems, conduction transfer function methodology is a commonly used solution technique, which most of the building energy analysis programs use. The equations given in Table 4 can be solved easily by fixed point iteration. The solution scheme is provided in Table 5.

RESULTS

Results from two experiments are used to investigate the applicability of the EMPD concept. The lumped energy and moisture transfer equations are solved to predict the weight change of an arm chair used in the first experiment. For the second experiment, the indoor conditions and the cooling loads of a night-ventilated test cell are predicted and compared to the measured values. The equilibrium sorption isotherm curves (Kerestecioglu, et al. 1988) of the materials used in the simulations are shown in Figure 3.

The arm chair was one of many samples used in the first experiment to explore the moisture behavior of common furniture and building materials. The specimens were kept in a conditioned space until they attained moisture equilibrium. The conditions in the space were then changed and the weight of the specimens were monitored accurately using precision load cells. Additionally, the space dry bulb and dew point temperatures were recorded. The arm chair is assumed to be composed mainly of wool and wood. Hence, its behavior is simulated using the sorption isotherms of each of these materials. In these simulations, the convective heat and mass transfer coefficients were assumed to be $3.0 \text{ W/m}^2\cdot\text{K}$ and $0.003 \text{ kg/m}^2\cdot\text{s}$, respectively. The measured surface area of the arm chair was 4.0 m^2 approximately. Figures 4 and 5 show the comparison between measured and predicted weight change histories for the arm chair using the sorption isotherms of wool and wood, respectively. It is evident from the figures that one can match the experimental data with different sets of sorption isotherm and EMPD. For example, EMPD of 2.0 mm and 1.4 mm are found to be the optimum values for wool and wood, respectively. The time taken by the lumped layer to reach equilibrium with the surroundings is a strong function of its moisture capacity. Smaller values of EMPD mean smaller moisture capacities and lead to quicker response and vice versa. Although results show that the optimum penetration depth varies with the sorption isotherm chosen, the "effective moisture capacities" ($A\rho_s\delta_M$) are almost identical in both cases. Therefore, density and surface area are also key parameters.

In Figures 6 through 8, data from a second experiment (Kamel et al. 1986) conducted at the Florida Solar Energy Center (FSEC) is used for comparison with results from simulation. In the experiment, two identically configured test rooms in FSEC's Passive Cooling Laboratory were used to determine the energy savings

due to night ventilation. The room used in the simulation was ventilated between the hours of 8 PM and 7 AM, and conditioned during the day by running a window type air conditioner. Materials participating in moisture transport were the gypsum walls, nylon carpet and linen furniture. The energy equation (Eq. 34) was solved using finite element method to get the temperature distribution through the walls, floor and window, while the lumped moisture equation (Eq. 5) was used for walls as well as furniture.

Figure 6 shows the comparison of measured and predicted values of temperature and humidity ratio for the zone air. Figure 7 shows predicted and measured inside surface temperatures for the window and ceiling of the test cell. In both figures optimized values of the EMPD were used. Different heat and moisture transport coefficients were used during ventilation and air-conditioning hours. Figure 8 shows the comparison of predicted and measured sensible and latent cooling loads for the room during the air-conditioning periods. The figure includes results of the simulation with and without the moisture effects of the participating materials. In load prediction, measured room temperatures served as inputs to the simulation. It is clear from the figure that the EMPD has a significant effect on the latent load and little effect on the sensible load prediction. Ignoring the moisture transport in building materials can lead to significant errors in latent load prediction.

CONCLUSIONS

EMPD is a viable concept that can be used in building energy analysis and easily incorporated into existing computer codes. For a given material, if the density, sorption isotherm and surface area are known, the only unknown parameter needed is the value of EMPD. The prediction of indoor conditions and associated loads are very sensitive to the value of EMPD. Ignoring moisture transport in

building materials can lead to errors in load and indoor condition predictions. Long time performances (when the inner regions of the material is affected) cannot be determined by a single value of EMPD. The concept must be used with caution and good judgement and must be backed by experimental data or detailed simulation to determine the range of applicability. Different EMPD values may be required for different operating conditions. These values can be determined from experiments or detailed simulations.

ACKNOWLEDGEMENTS

The work reported here is funded under GRI contract #5087-243-1515 with the Gas Research Institute, 860 West Bryn Mawr Ave., Chicago, Illinois, and DOE cooperative agreement #DE-FC03-865F16305 with the Department of Energy San Francisco Operations Office, 1333 Broadway, Oakland, California. The authors thank Doug Kosar of GRI and David Pellish of DOE-Solar for their continued support of this research. The authors also thank Philip Fairey and Subrato Chandra for helpful discussions.

NOMENCLATURE

A	Heat and moisture transfer surface area [m ²]
a _T	Solution vector to Eq. (10) [K]
C _p	Specific heat [J/kg.K]
D _v	Total moisture diffusivity [m ² /s]
EI	Rate of air leaving the "zone" by infiltration [1/s]
EM	Rate of air leaving the "zone" by internal air flows [1/s]
EV	Rate of air leaving the "zone" by ventilation [1/s]
fc	Ratio of convective heat to total sensible heat from lights
h _M	Convective mass transfer coefficient [kg/m ² .s]
h _T	Convective heat transfer coefficient [W/m ² .K]
i	Summation index over surface number one
II	Rate of air coming to the "zone" by infiltration [1/s]
IM	Rate of air coming to the "zone" by internal air flows [1/s]
IV	Rate of air coming to the "zone" by ventilation [1/s]
k	Thermal conductivity [W/m.K]
L	Length [m]
m	Mass flow rate of the supply air [kg/s]
nof	Number of furniture lumps in the "zone"
nos	Number of internal heat transfer surfaces in the "zone"
noz	Number of "zones" to be simulated simultaneously
Np	Number of people in the "zone"
q ["] _M	Imposed moisture flux [kg/m ² .s]
q ["] _T	Imposed heat flux [W/m ²]

R_v Ideal gas constant [461.52 J/kg.K]
 R_e Ratio of radiative heat to total sensible heat from equipment
 R_p Ratio of radiative heat to total sensible heat from people
 T Temperature [K]
 T_j Temperature of the other surface [K]
 T_o Ventilation air outlet temperature [K]
 T_r "Zone" air dry-bulb temperature [K]
 T_{ro} Initial "zone" air temperature [K]
 T_s Radiation receiver temperature [K]
 U Moisture content (dry basis) [kg/kg]
 U_e Equipment utilization coefficient
 U_l Lighting utilization coefficient
 V Volume of the "zone" [m³]
 W Humidity ratio [kg/kg]
 W_{e-l} Latent heat gain from equipment [W]
 W_{e-s} Sensible heat gain from equipment [W]
 W_l Sensible heat gain from light [W]
 W_{p-l} Latent heat gain from people [W]
 W_{p-s} Sensible heat gain from people [W]
 W_r Humidity ratio of the "zone" air [kg/kg]
 W_{ro} Initial "zone" air-humidity ratio [kg/kg]
 δ_M Penetration depth for the moisture equation [m]
 δ_T Penetration depth for the energy equation [m]
 ϵ Emissivity or error tolerance
 ϵ_v Ventilation air mixing efficiency factor
 λ Heat of vaporization [J/kg]
 ρ Density [kg/m³]
 σ Stefan-Boltzmann constant [W/m².K⁴]
 τ Time [h]
 ϕ Relative humidity [0 to 1]

SUBSCRIPTS AND SUPERSSCRIPTS

a Air
 s Solid
 sat Saturation
 sup Supply air
 α Ambient
 * Surface condition

REFERENCES

- Burch, D. 1985. "Experimental Validation of a Mathematical Model for Predicting Moisture in Attics." in Moisture and Humidity, Measurement and Control in Science and Industry, Proceedings of the 1985 International Symposium on Moisture and Humidity, Washington, D.C., pp. 287-296.
- Cleary, P.; and Sonderegger, R. 1984. "A Method to Predict the Hour by Hour Humidity Ratio in Attic Air." Presented at the ASTM Symposium on Thermal Insulation, Materials and Systems, Dallas, Texas, Dec. 2-6.
- Cleary, P.G. 1985. "Moisture Control by Attic Ventilation - An In Situ Study." ASHRAE Paper No. 2872, ASHRAE Winter Meeting, Chicago.

- Cleary, P.; and Sherman, M. 1985. "Seasonal Storage of Moisture in Roof Sheathing." in Moisture and Humidity, Measurement and Control in Science and Industry, Proceedings of the 1985 International Symposium on Moisture and Humidity, Washington, D.C., pp. 313-323.
- Cunningham, M.J. 1983(a). "A New Analytical Approach to the Longterm Behavior of Moisture Concentrations in Building Cavities - I. Non-Condensing Cavity." Building and Environment, Vol. 18, No. 3, pp. 109-116.
- Cunningham, M.J. 1983(b). "A New Analytical Approach to the Longterm Behavior of Moisture Concentrations in Building Cavities - II. Condensing Cavity." Building and Environment, Vol. 18, No. 3, pp. 117-124.
- Cunningham, M.J. 1984. "Further Analytical Studies of Building Cavity Moisture Concentrations." Building and Environment, Vol. 19, No. 1, pp. 21-29.
- Cunningham, M.J. 1985. "Automatic Datalogging Timber Moisture Contents Over the Range 10% - 50% w/w." Moisture and Humidity 1985, Proceedings of the 1985 International Symposium on Moisture and Humidity, Washington, D.C.
- Cunningham, M.J. 1988. "The Moisture Performance of Framed Structures - A Mathematical Model." Building and Environment, Vol. 23, No. 2, pp. 123-135.
- Kamel, A.; Fairey, P.; Kerestecioglu, A; and Chandra, S. 1986. "Experimental Determination of Ventilative Cooling Energy Savings." FSEC-CR-161-86.
- Kerestecioglu, A.; Swami, M.; Dabir, R.; Razzaq, N.; and Fairey, P. 1988. "Theoretical and Computational Investigation of Algorithms for Simultaneous Heat and Moisture Transport in Buildings." FSEC-CR-191-88.
- Kerestecioglu, A.; Fairey, P.; and Chandra, S. 1985. "Algorithms to Predict Detailed Moisture Effects in Buildings." Proceedings, Thermal Performance of The Exterior Envelopes of Buildings III, ASHRAE/DOE/BTECC Conference, Clearwater Beach, FL.
- Kusuda, T. 1983. "Indoor Humidity Calculations." ASHRAE Transactions, Vol. 89, Part 2.B, pp. 728-740.
- Kusuda, T.; and Miki, M. 1985. "Measurement of Moisture Content for Building Interior Surfaces." in Moisture and Humidity, Measurement and Control in Science and Industry, Proceedings of the 1985 International Symposium on Moisture and Humidity, Washington, D.C., pp. 297-311.
- Ortega, J.M.; and Rheinboldt, W.C. 1980. Iterative Solution of Nonlinear Equations in Several Variables, New York: Academic Press.

TABLE 1

Building Domains, Boundaries and their Characteristics

SYMBOL	CONTENT	CHARACTERISTICS
Ω_e	Envelope	Identifiable geometries and possibly known material properties.
Ω_a	Zone air surrounded by envelope	Identifiable geometry and well known material properties.
Ω_f	Internal mass and furniture	Irregular geometries and hard to define material properties.
Γ_e	Exterior surface of the envelope	Separates envelope from ambient
Γ_a	Interior surface of the envelope	Separates the envelope from the zone air.
Γ_f	Exterior surface of the furniture	Separates the internal mass and furniture from the zone air.

TABLE 2

Zone Energy Balance Components

Term	Description	Equation
Q _{equ-s}	Energy gains from equipment	$Ue_i - We-s_i (1-Re_i)$
Q _{fur-s}	Energy absorbed or released by furniture	$\sum_{k=1}^{nof} h_{Ti,k} A_{i,k} (T_{i,k}^* - Tr_i)$ on Γ_f
Q _{inf-s}	Energy gain or loss due to infiltration	$V_i (II_i \rho_a C_p T_\alpha - EI_i \rho_a C_p Tr_i)$
Q _{lig-s}	Convective energy gains from lighting	$Ul_i - Wl_i - fc_i$
Q _{mix-s}	Energy added or removed by internal flows	$V_i \left(\sum_{j=1}^{noz} IM_{i,j} \rho_a C_p Tr_j - \sum_{j=1}^{noz} EM_{i,j} \rho_a C_p Tr_i \right)$
Q _{peo-s}	Convective gain from occupants	$Np_i - Wp-s_i (1 - Rp_i)$
Q _{sin-s}	Energy removed by sinks	Functional definition
Q _{son-s}	Energy added by sources	Functional definition
Q _{sup-s}	Energy added or removed by supply air	$m'_{i,s} C_p (T_{sup,i} - Tr_i)$
Q _{ven-s}	Energy gain or loss due to ventilation	$\epsilon_v V_i (IV_i \rho_a C_p T_\alpha - EV_i \rho_a C_p Tr_i)$
Q _{wal-s}	Energy flow between zone and interior envelope surfaces	$\sum_{k=1}^{nos} h_{Ti,k} A_{i,k} (T_{i,k}^* - Tr_i)$ on Γ_a

TABLE 3

Zone Moisture Balance Components

Term	Description	Equation
Qcon-1	Moisture condensation	$\sum_{k=1}^{nos} h_{Mi,k} A_{i,k} (W_{r_i} - W_{i,k}^*)$
Qequ-1	Moisture gains from equipment	$Ue_i W_{e-1_i} / \lambda$
Qfur-1	Moisture adsorbed or desorbed by furniture	$\sum_{k=1}^{nof} h_{Mi,k} A_{i,k} (W_{i,k}^* - W_{r_i}) \text{ on } \Gamma_F$
Qinf-1	Moisture added or removed by infiltration	$V_i (II_i \rho_a W_\alpha - EI_i \rho_a W_{r_i})$
Qmix-1	Moisture added or removed by internal flows	$V_i \left(\sum_{j=1}^{nos} IM_{i,j} \rho_a W_{r_j} - \sum_{j=1}^{nos} EM_{i,j} \rho_a W_{r_i} \right)$
Qpeo-1	Moisture gain from occupants	$Np_i W_{p-1_i} / \lambda$
Qrev-1	Moisture due to reevaporation	$m^* (W_{sup,i} - W_{r_i})$
Qsin-1	Moisture removed by sinks	Functional definition
Qsor-1	Moisture added by sources	Functional definition
Qsup-1	Moisture removed by supply air	$m^*_i (W_{sup,i} - W_{r_i})$
Qven-1	Moisture added or removed by ventilation	$\epsilon_V V_i (IV_i \rho_a W_\alpha - EV_i \rho_a W_{r_i})$
Qwal-1	Moisture adsorbed or desorbed by envelope	$\sum_{k=1}^{nos} h_{Mi,k} A_{i,k} (W_{i,k}^* - W_{r_i}) \text{ on } \Gamma_a$

TABLE 4

Variables to be Calculated and Their Requirements

VARIABLE TO BE CALCULATED	REQUIREMENTS
Tr in Ω_a from Eq. (1)	1) T^* on Γ_a from Eq. (10) 2) T^* on Γ_f from Eq. (4)
Wr in Ω_a from Eq. (2)	1) W^* on Γ_a from Eq. (5) 2) W^* on Γ_f from Eq. (5)
T^* in Ω_f from Eq. (4)	1) Tr in Ω_a from Eq. (1) 2) Wr in Ω_a from Eq. (2) 3) W^* on Γ_f from Eq. (5)
W^* in Ω_e and Ω_f from Eq. (5)	1) Wr in Ω_a from Eq. (2) 2) T^* on Γ_a from Eq. (10) 3) T^* on Γ_e from Eq. (10) 4) T^* on Γ_f from Eq. (4) 5) Relations given by Eqs. (6) - (8)
T^* on Γ_a and Γ_e from Eq. (10)	1) Tr in Ω_a from Eq. (1) 2) Wr in Ω_a from Eq. (2) 3) W^* on Γ_a from Eq. (5) 4) W^* on Γ_e from Eq. (5)

TABLE 5

Fixed Point Iteration Scheme

- <1> Guess $Tr_n^{\tau+\Delta\tau}$, $Wr_n^{\tau+\Delta\tau}$, $W_n^{\tau+\Delta\tau}$, $T_n^{\tau+\Delta\tau}$ and $a_{T,n}^{\tau+\Delta\tau}$
- <2> With known $Tr_n^{\tau+\Delta\tau}$ and $Wr_n^{\tau+\Delta\tau}$ solve Eqs. (14), (15) and (16). Get $W_{n+1}^{\tau+\Delta\tau}$ and $T_{n+1}^{\tau+\Delta\tau}$
- <3> With known $W_{n+1}^{\tau+\Delta\tau}$ solve Eq. (10) and get $a_{T,n+1}^{\tau+\Delta\tau}$ and $T_{n+1}^{\tau+\Delta\tau}$
- <4> With known $T_{n+1}^{\tau+\Delta\tau}$ and $W_{n+1}^{\tau+\Delta\tau}$ solve Eqs. (12) and (13). Get $Tr_{n+1}^{\tau+\Delta\tau}$ and $Wr_{n+1}^{\tau+\Delta\tau}$
- <5> Check for convergence

$$|Tr_{n+1}^{\tau+\Delta\tau} - Tr_n^{\tau+\Delta\tau}| < \epsilon \quad |Wr_{n+1}^{\tau+\Delta\tau} - Wr_n^{\tau+\Delta\tau}| < \epsilon$$

$$|W_{n+1}^{\tau+\Delta\tau} - W_n^{\tau+\Delta\tau}| < \epsilon \quad |T_{n+1}^{\tau+\Delta\tau} - T_n^{\tau+\Delta\tau}| < \epsilon$$

$$|a_{T,n+1}^{\tau+\Delta\tau} - a_{T,n}^{\tau+\Delta\tau}| < \epsilon$$

- <6> If the solution converges increment the time $\tau+\Delta\tau$ and go to step <1>
- <7> If the solution does not converge relax the solution as follows:

$$Tr_{n+1}^{\tau+\Delta\tau} = \mathcal{R} Tr_{n+1}^{\tau+\Delta\tau} + (1-\mathcal{R}) Tr_n^{\tau+\Delta\tau}$$

$$Wr_{n+1}^{\tau+\Delta\tau} = \mathcal{R} Wr_{n+1}^{\tau+\Delta\tau} + (1-\mathcal{R}) Wr_n^{\tau+\Delta\tau}$$

$$W_{n+1}^{\tau+\Delta\tau} = \mathcal{R} W_{n+1}^{\tau+\Delta\tau} + (1-\mathcal{R}) W_n^{\tau+\Delta\tau}$$

$$T_{n+1}^{\tau+\Delta\tau} = \mathcal{R} T_{n+1}^{\tau+\Delta\tau} + (1-\mathcal{R}) T_n^{\tau+\Delta\tau}$$

$$a_{T;n+1}^{\tau+\Delta\tau} = \mathcal{R} a_{T;n+1}^{\tau+\Delta\tau} + (1-\mathcal{R}) a_{T,n}^{\tau+\Delta\tau}$$

- <8> Update the variables and go to step <2>

Note: n denotes the iteration number, ϵ denotes the error tolerance, and \mathcal{R} is the relaxation parameter.

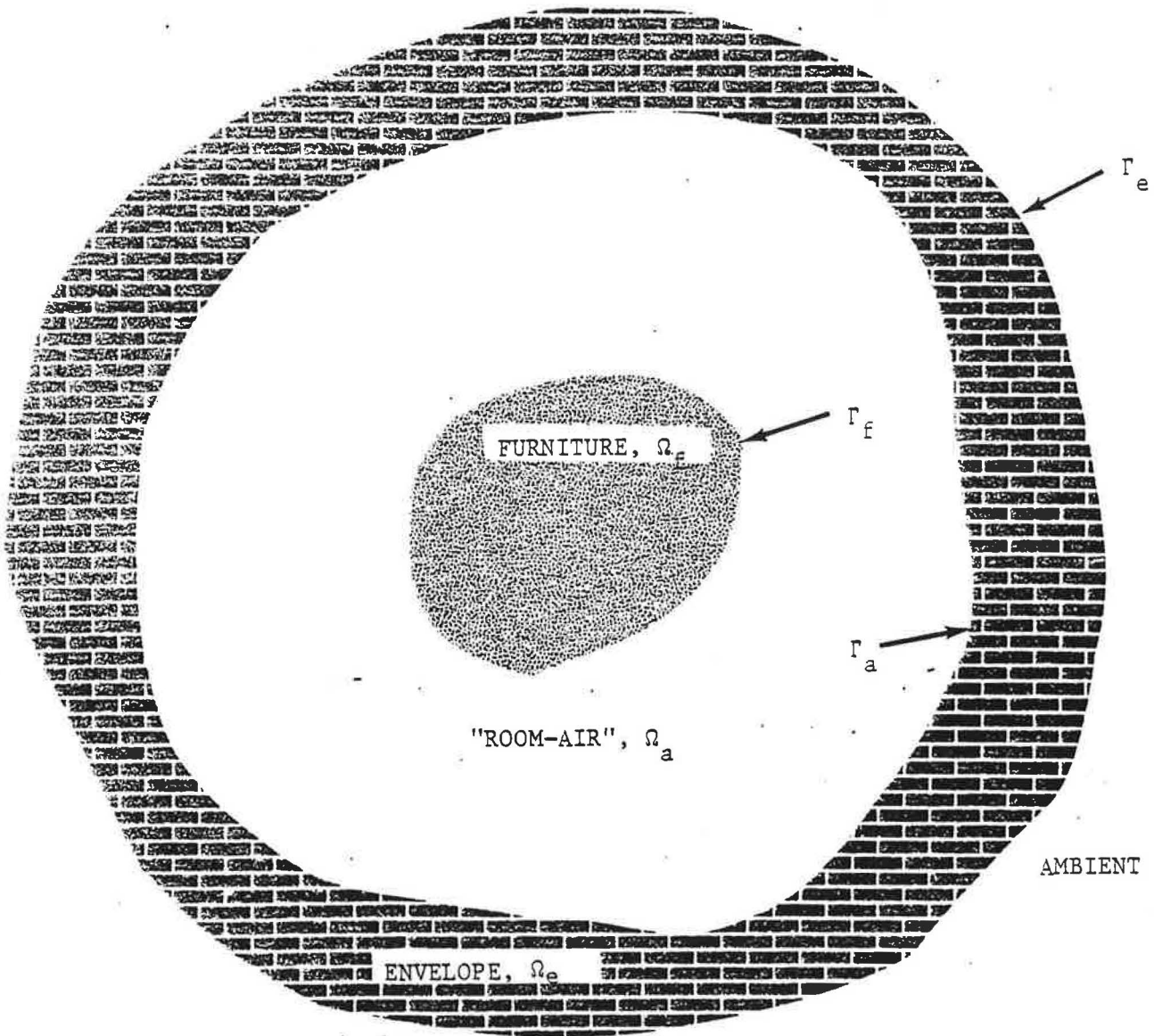


Figure 1. Building domains and boundaries.

10

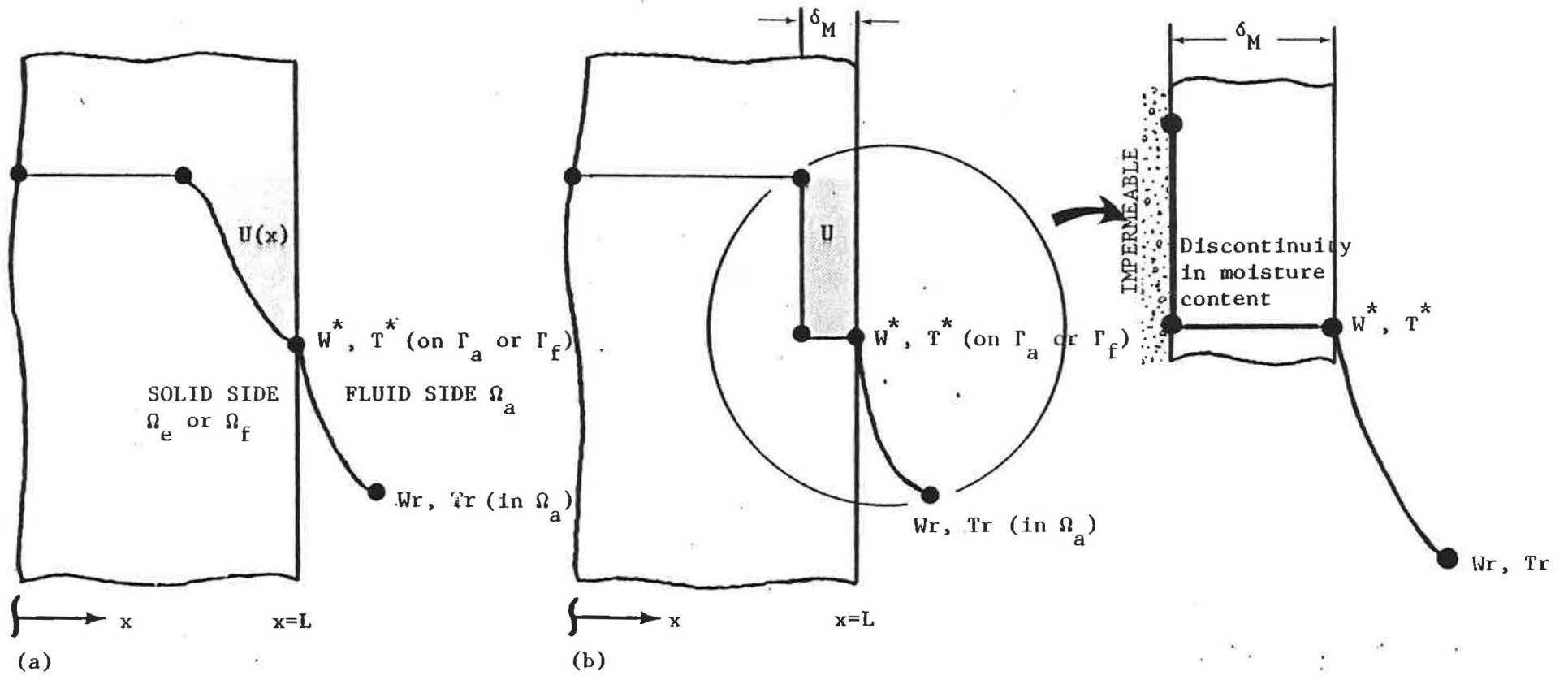


Figure 2. Schematics of "effective penetration depth" concept. (a) "Real moisture content gradient profile, $U(x)$; Lumped moisture content profile, U .

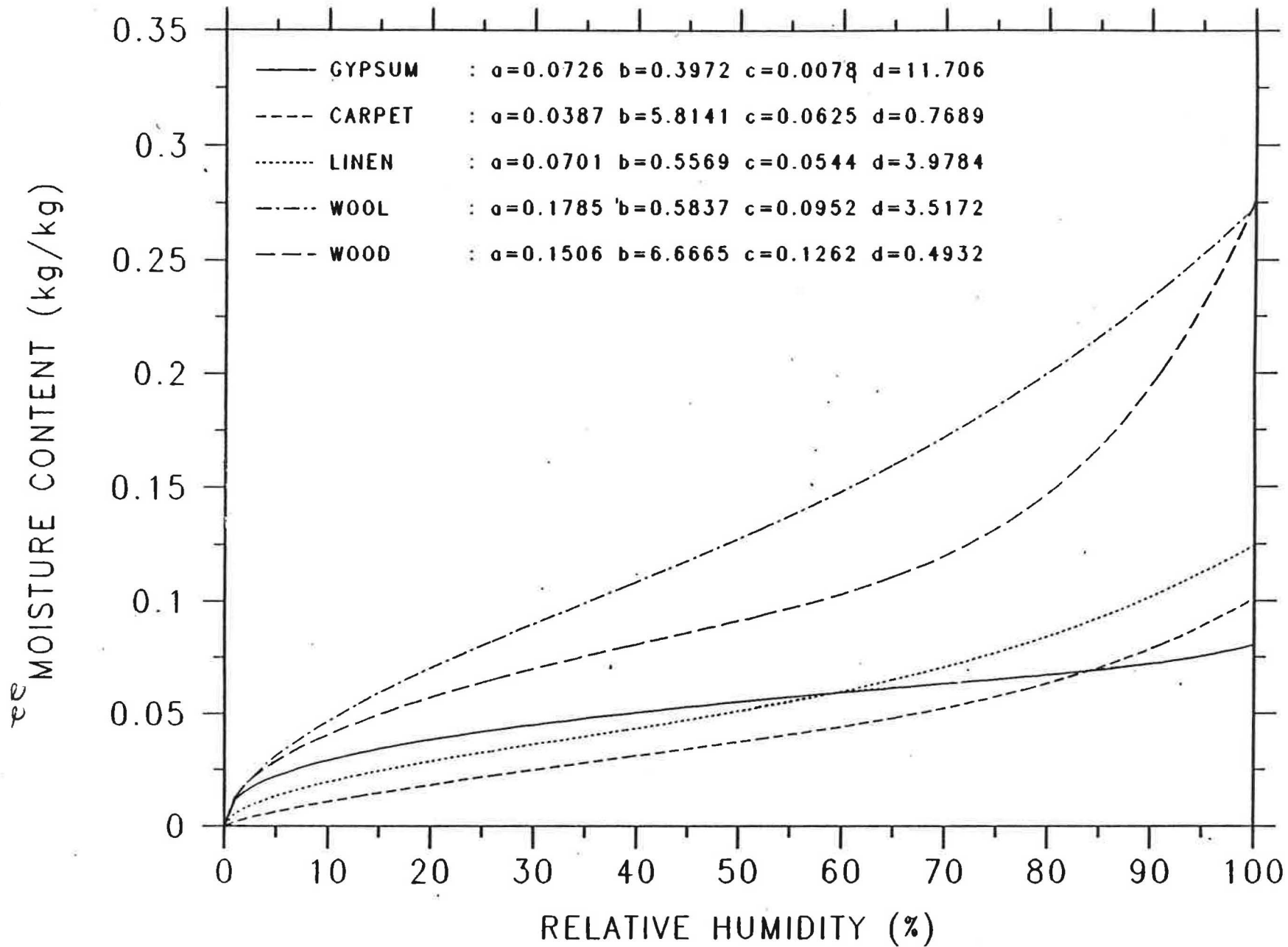


Figure 3. Sorption isotherms used in the simulations (Kerestecioglu et al. 1988).

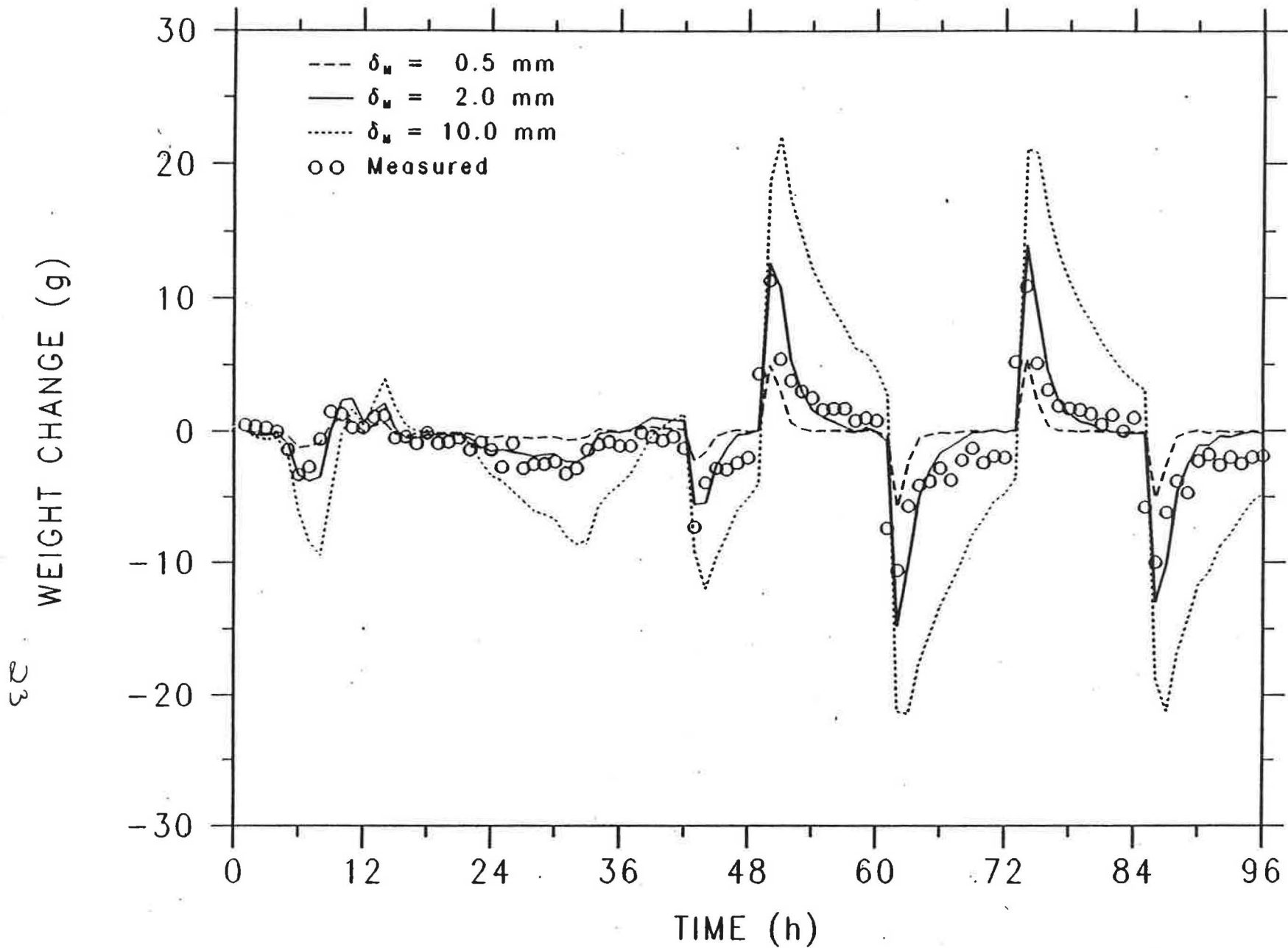


Figure 4. Effect of "effective penetration depth" on the weight change history of an arm chair using "wool" sorption data.

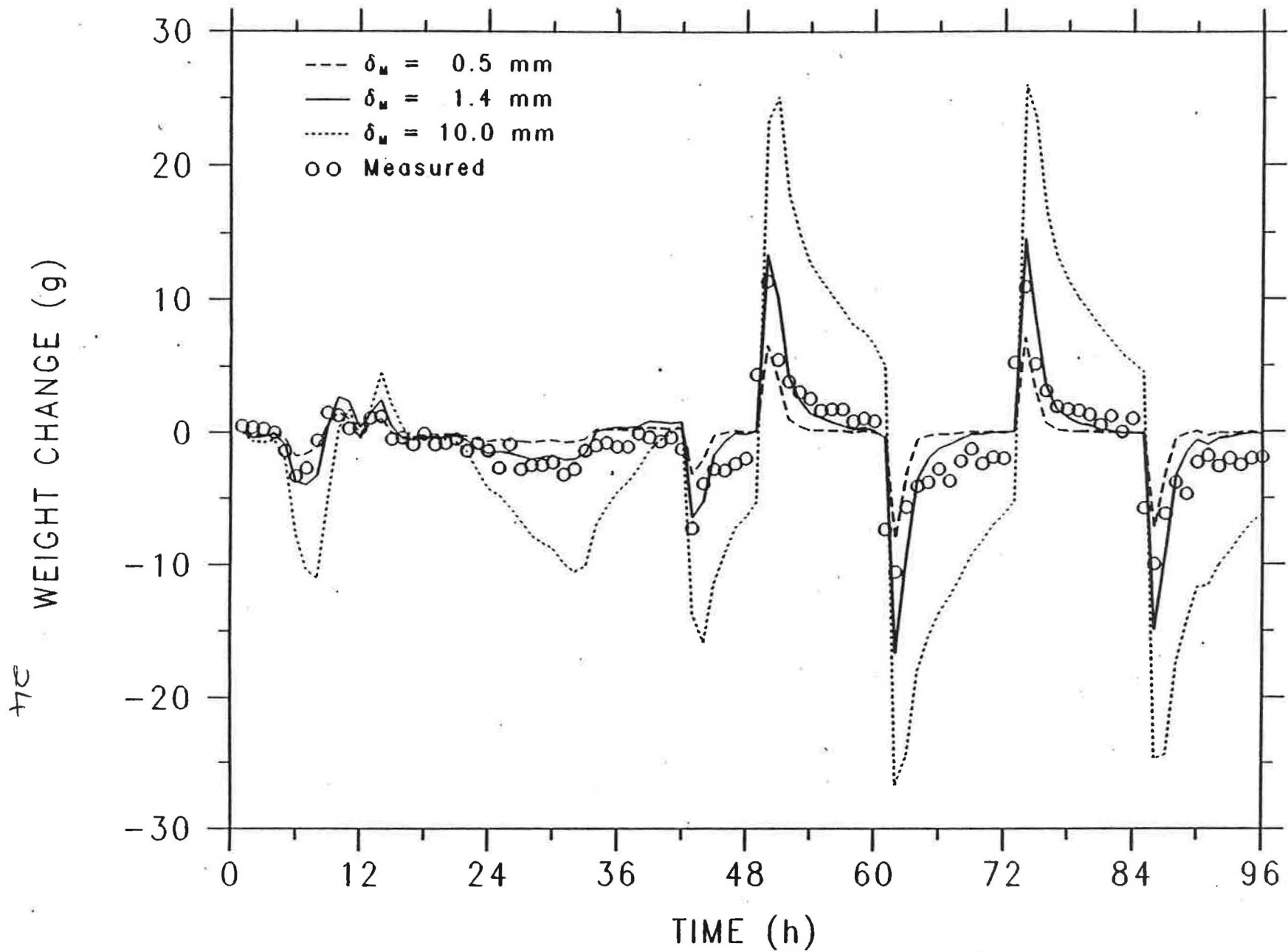


Figure 5. Effect of "effective penetration depth" on the weight change history of an arm chair using "wood" sorption data.

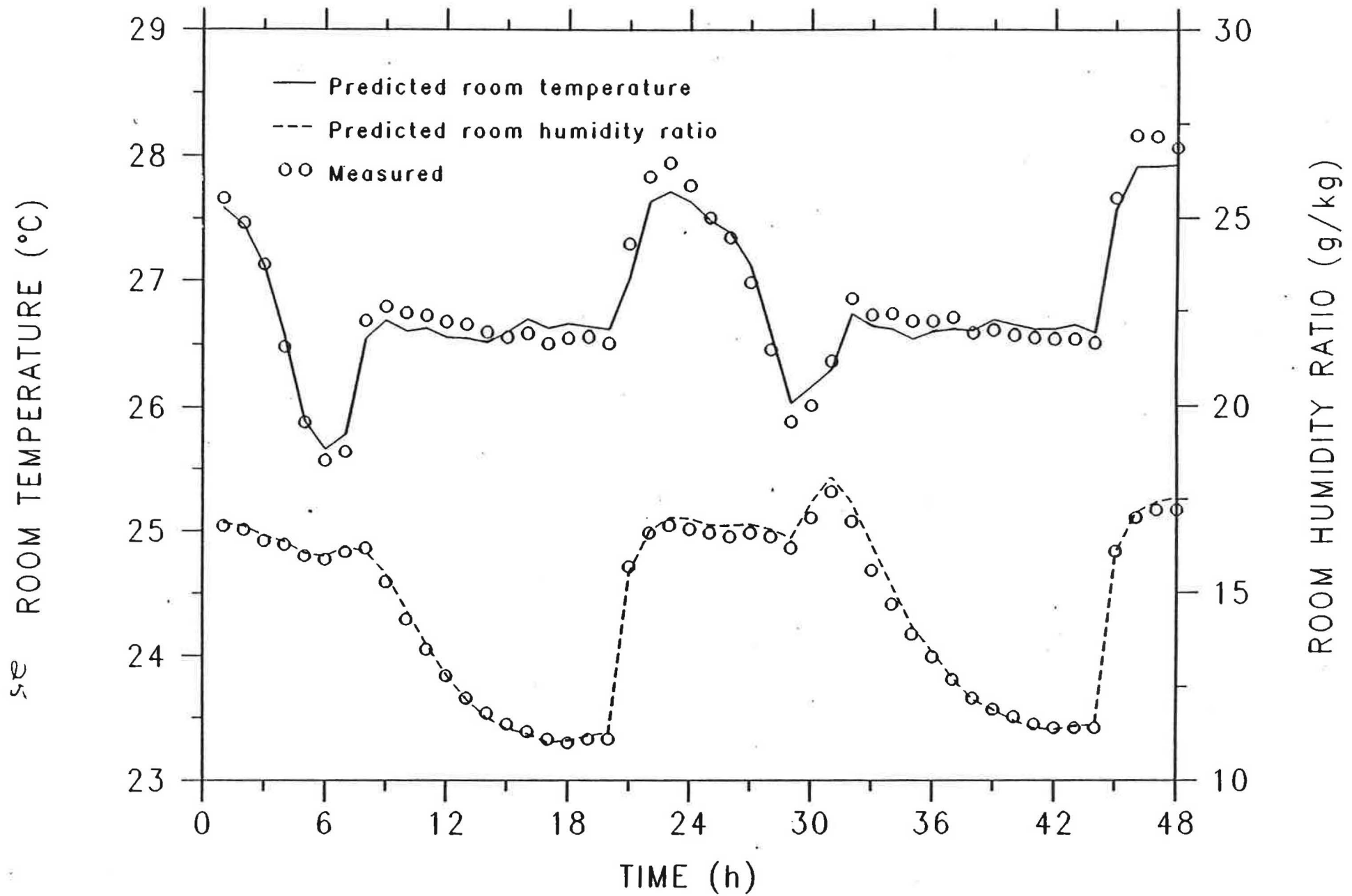


Figure 6. Comparison of predicted and measured room temperatures and humidity ratios.

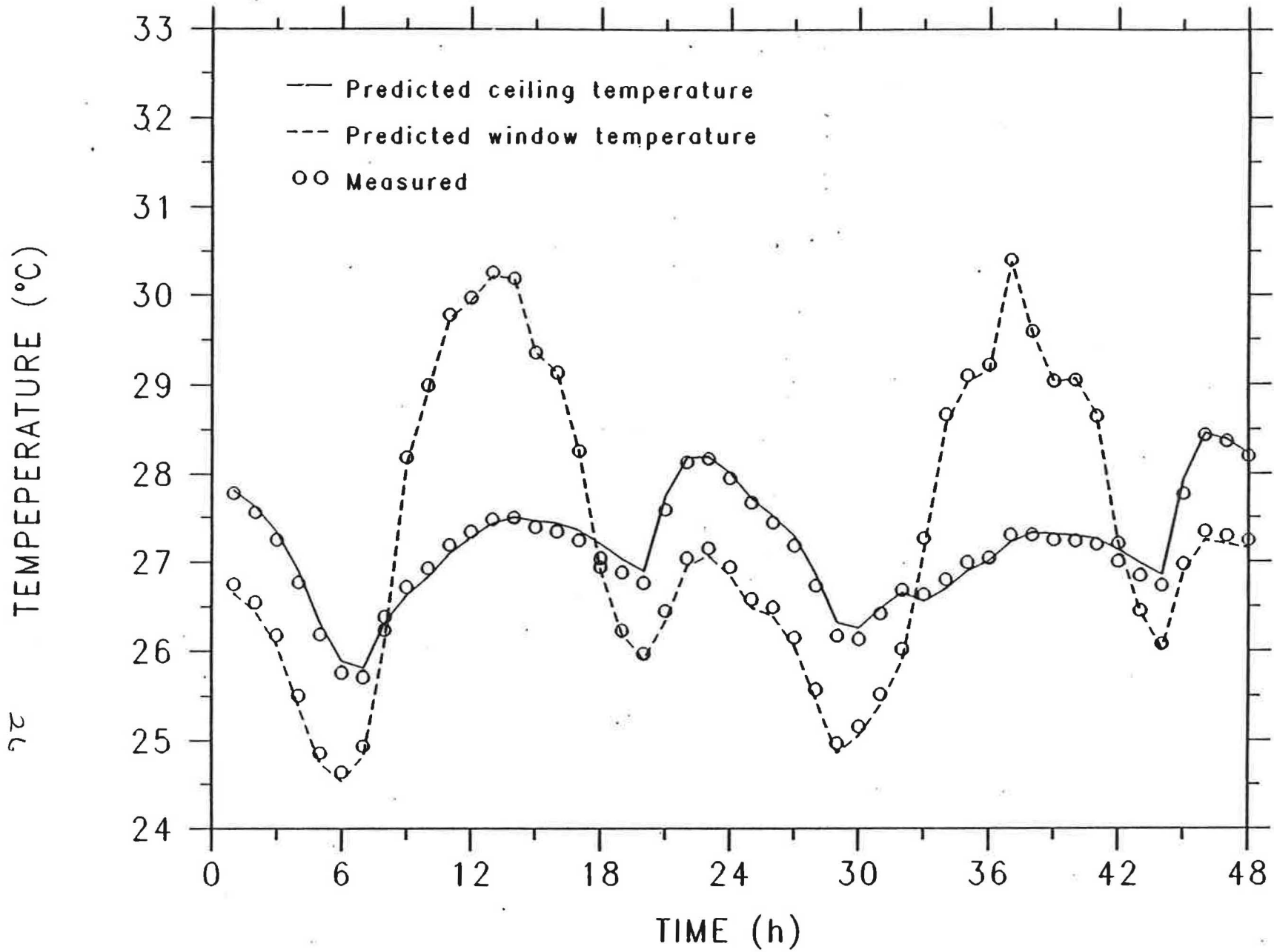


Figure 7. Comparison of predicted and measured surface temperatures.

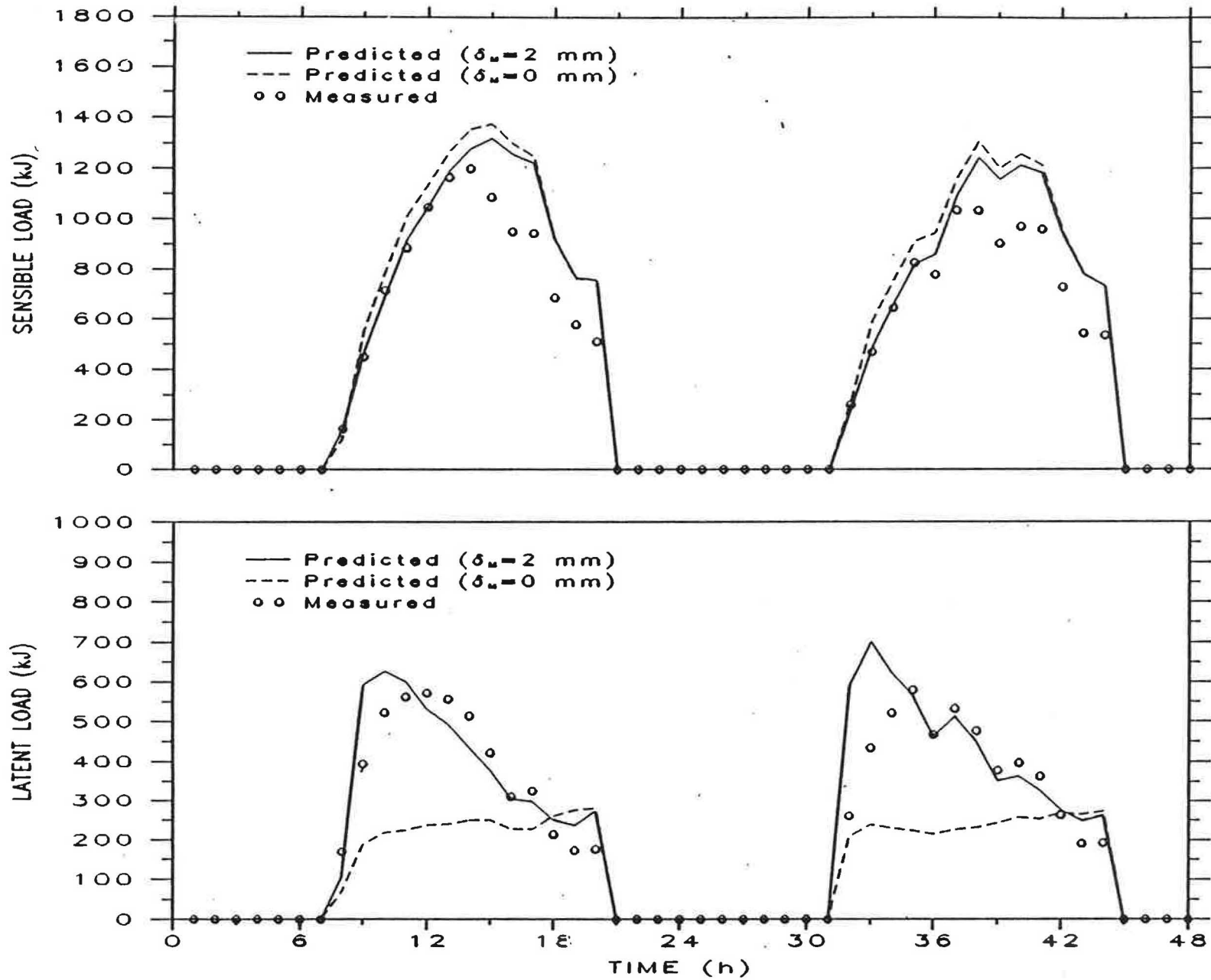


Figure 8. Comparison of predicted and measured room sensible and latent loads.